European Journal of Pharmacology 985 (2024) 177073

Contents lists available at ScienceDirect

European Journal of Pharmacology

journal homepage: www.elsevier.com/locate/ejphar

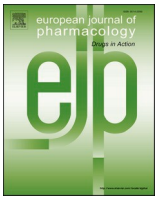

Dantrolene paradoxically exacerbates short-term brain glucose hypometabolism, hippocampal damage and neuroinflammation induced by status epilepticus in the rat lithium-pilocarpine model

Luis García-García [a,b,e,*], Francisca Gómez-Oliver [a,b,e], Rubén Fernández de la Rosa [b,c], Miguel Ángel Pozo [b,d,e]

[a] Department of Pharmacology, Pharmacognosy and Botany. Faculty of Pharmacy, Complutense University of Madrid, Madrid, Spain
[b] Brain Mapping Unit, Instituto Pluridisciplinar, Complutense University of Madrid, Madrid, Spain
[c] ICTS Bioimagen Complutense (BIOIMAC), Complutense University of Madrid, Madrid, Spain
[d] Department of Physiology, Faculty of Medicine, Complutense University of Madrid, Madrid, Spain
[e] Health Research Institute, Hospital Clínico San Carlos (IdISSC), Madrid, Spain

ARTICLE INFO

Keywords:
Lithium-pilocarpine model
Status epilepticus
Dantrolene
PET
Brain glucose metabolism
Neuroprotection

ABSTRACT

Status epilepticus (SE) is a neurologic emergency characterized by prolonged or rapidly recurring seizures. Increased intracellular calcium concentration ($[Ca^{2+}]_i$) occurring after SE is a key mediator of excitotoxicity that contributes to the brain damage associated with the development of epilepsy. Accumulated evidence indicates that dantrolene, a ryanodine receptor (RyR) blocker may have protective effects against the SE-induced damage. We evaluated whether dantrolene (10 mg/kg, i.p.) administered twice, 5 min and 24 h after the lithium-pilocarpine-induced SE in rats, had neuroprotective effects. Dantrolene by itself had no effects on control rats. However, it exacerbated the signs of damage in rats that underwent SE, increasing brain glucose hypometabolism as measured by PET neuroimaging 3 days after SE. Likewise, the neurohistochemical studies revealed that dantrolene aggravated signs of hippocampal neurodegeneration, neuronal death and microglia-induced neuroinflammation. Besides, the damaging effects were reflected by severe body weight loss. Overall, our results point towards a deleterious effect of dantrolene in the lithium-pilocarpine-induced SE model. Nonetheless, our results are in opposition to the reported neuroprotective effects of dantrolene. Whether the mechanisms underlying $[Ca^{2+}]_i$ increase might significantly differ depending on the particularities of the model of epilepsy used and general experimental conditions need further studies. Besides, it is yet to be determined which isoform of RyRs significantly contributes to Ca^{2+}-induced excitotoxicity in the lithium-pilocarpine SE rat model.

1. Introduction

Epilepsy is one of the most common chronic neurological disorders characterized by a persistent drift to generate spontaneous seizures and by its disabling consequences (Fisher et al., 2017). Among the types of epilepsy, temporal lobe epilepsy (TLE) is the most predominant focal epilepsy in adults, being highly refractory to the current pharmacotherapy (Tang et al., 2017). TLE is accompanied by hippocampal sclerosis (Janszky et al., 2005) and interictal glucose hypometabolism in the epileptogenic focus (Kumar and Chugani, 2017a, 2017b). The latter can be efficiently evaluated by 2-deoxy-2-[^{18}F]fluoro-D-glucose ([^{18}F]FDG) positron emission tomography (PET) neuroimaging. Furthermore, in TLE patients, interictal focal hypometabolism is one of the best early biomarkers of epilepsy (O'Brien et al., 2008).

One of the most used animal models of epilepsy is the lithium-pilocarpine rat model of status epilepticus (SE) (Ahmed Juvale and

Abbreviations: AD, Alzheimer's disease; BW, Body weight; [^{18}F]FDG, 2-deoxy-2-[^{18}F]fluoro-D-glucose; ER, Endoplasmic reticulum; GFAP, Glial fibrillary acidic protein; IP_3, Inositol 1,4,5-tris-phosphate; IP_3R, IP_3 receptor; MRI, Magnetic resonance imaging; NMDA, N-methyl-d-aspartate; NMDAR, NMDA receptor; PET, Positron emission tomography; RyR, Ryanodine receptor; SE, Status epilepticus; SERCA, Sarco/endoplasmic reticulum calcium ATPase; TLE, Temporal lobe epilepsy; TSPO, Translocator protein 18 kDa.

* Corresponding author. Unidad de Cartografía Cerebral, Instituto Pluridisciplinar, Universidad Complutense de Madrid, Paseo Juan XXIII n 1, 28040, Madrid, Spain.
E-mail address: lgarciag@ucm.es (L. García-García).

https://doi.org/10.1016/j.ejphar.2024.177073
Received 8 August 2024; Received in revised form 23 September 2024; Accepted 28 October 2024
Available online 29 October 2024

Che Has, 2020). This model reproduces many features of human TLE (Brandt et al., 2015; Turski et al., 1983). The SE induced by pilocarpine is followed by a latent (or silent) period (Pitkänen, 2002) that is characterized by generalized brain hypometabolism (García-García et al., 2023; Lee et al., 2012). Brain hypometabolism is accepted as an early marker of epileptogenesis (Zhang et al., 2015) that occurs concurrently with neurodegeneration, neuronal death, neuroinflammation and reactive gliosis (García-García et al., 2023; Rossi et al., 2013). Brain hypometabolism has been attributed, among others, to neuronal death, reduction in synaptic density (Kumar and Chugani, 2017a, 2017b), and cerebral hypoperfusion (Bascuñana et al., 2021).

Epileptogenic activity is also associated with abnormally elevated intracellular Ca^{2+} concentrations ($[Ca^{2+}]_i$) which is a key mediator that contributes ultimately to the excitotoxic damage, being excitotoxicity one of the main mechanisms underlying neuronal cell death and plasticity changes associated with the development of epilepsy (Steinlein, 2014). Studies in the pilocarpine model have revealed that SE increases $[Ca^{2+}]_i$ in the CA1 hippocampal neurons, that remain high afterwards (Raza et al., 2001, 2004). Rise in $[Ca^{2+}]_i$ involves N-methyl-d-aspartate (NMDA) receptor (NMDAR) activation (DeLorenzo et al., 1998; Rice and Delorenzo, 1998), inhibition of sarco/endoplasmic reticulum calcium ATPase (SERCA) activity and increased activities of the inositol 1,4,5-tris-phosphate (IP_3) receptor (IP_3R) (Pal et al., 2001) and the ryanodine receptor (RyR) (Nagarkatti et al., 2010; Niebauer and Gruenthal, 1999; Yoshida and Sakai, 2006).

Dantrolene is an RyR antagonist that at high doses also blocks NMDAR (Obenaus et al., 1989; Salinska et al., 2008). Dantrolene is currently approved for the treatment of malignant hyperthermia (Yang et al., 2023).

Regarding excitotoxicity, dantrolene suppresses neuronal injury induced by metabotropic glutamate receptor activation in neonatal rats (McDonald et al., 1993) and neuroprotective effects have been reported in some models of SE (Mori et al., 2005; Niebauer and Gruenthal, 1999).

No studies have been reported evaluating the potential neuroprotective effects of dantrolene in the rat lithium-pilocarpine model of SE, much less on its effects on brain metabolic activity. Accordingly, we have evaluated the short-term effects of post-SE dantrolene administration on brain glucose metabolism by [^{18}F]FDG PET and on histochemical markers of neuroprotection and neuroinflammation.

2. Materials and methods

2.1. Animals

A total of 44 adult male Sprague-Dawley rats (Charles River Laboratories Spain) weighing 288.9 ± 5.6 g at the beginning of the study were used. Rats were housed in standard rat cages (2 rats/cage), on a ventilated rack (Tecniplast, Italy) under controlled conditions of temperature (22 ± 2 °C) and lighting (12 h light/dark cycle; 8:00 a.m.-8:00 p.m.). During the acclimation period as well as during the experimental procedure, rats had *ad libitum* access to standard rodent food, except for the 12h before the PET scans. The study was approved by the Animal Research Ethical Committee of the Universidad Complutense de Madrid and by the Autonomous Community of Madrid (PROEX 222.1/20), and it was conducted in accordance with regulations of the European Union (2010/63/UE) and Spain (RD53/2013) regarding animal welfare. All efforts were made to minimize, as much as possible, both the number of animals used and their suffering.

2.2. Lithium-pilocarpine rat model of SE

The procedure has been previously reported (García-García et al., 2023). Briefly, lithium chloride (LiCl) was administered (127 mg/kg i.p., Sigma–Aldrich) 18–20 h before the induction of SE by pilocarpine. Thirty minutes before pilocarpine injection (25 mg/kg, i.p.; Sigma–Aldrich, St. Louis, MO), rats were pre-treated with methyl-scopolamine (2 mg/kg, i.p.) to minimize the peripheral cholinergic effects. The dose of 25 mg/kg of pilocarpine was selected based on previous studies of our group as well as by other research groups (Rigoulot et al., 2004; Walton and Treiman, 1988; Yang et al., 2014).

According to the Racine scale, the onset of SE was considered when the animal reached the stage 4 (rearing with forelimb clonus) and showed continuous seizure activity (Racine, 1972). After 45 min, the seizure state was interrupted by administering pentobarbital (25 mg/kg, i.p.). The pilocarpine-treated rats that did not reach SE were discarded from the experiment. Control rats went through to the same administration schedule, but 1 ml/kg saline solution (SAL) was used instead of drugs.

2.3. Dantrolene administration

Dantrolene (Sigma-Aldrich, St. Louis, MO) was intraperitoneally administered at a dose of 10 mg/kg dissolved in distilled water, pH = 9.3. Dantrolene was administered twice, 5 min after the SE induced by pilocarpine and 24h after the SE. The dose of dantrolene was selected based on previous studies on rats (Berg et al., 1995; Niebauer and Gruenthal, 1999; Popescu et al., 2002; Yoshida and Sakai, 2006).

The initial experimental groups were as follows: (1) control rats (SAL + VEH group, n = 8); (2) rats injected with pilocarpine (PILO + VEH group, n = 14); (3) rats injected with dantrolene (SAL + DANT group, n = 8) and (4) rats injected with both pilocarpine and dantrolene (PILO + DANT, n = 14). Some rats died within the 24h after either pilocarpine and/or dantrolene administration rendering the following groups: (1) control rats (SAL + VEH group, n = 8); (2) rats injected with pilocarpine (PILO + VEH group, n = 12); (3) rats injected with dantrolene (SAL + DANT group, n = 6) and (4) rats injected with both pilocarpine and dantrolene (PILO + DANT, n = 8). Three days after pilocarpine (or saline) injection, brain glucose metabolism was evaluated by *in vivo* [^{18}F]FDG PET.

2.4. Body weight (BW) measurements

Rats were weighted at 6 time points during the experimental procedures: (i) initial BW, 24h before pilocarpine administration; (ii) at the moment of pilocarpine injection; (iii) 24h after pilocarpine administration; (iv) 48h after pilocarpine administration; (v) 72h after pilocarpine administration, at the moment of PET neuroimaging and (vi) 96h after pilocarpine administration on the day of sacrifice. Rats were sacrificed by decapitation and brains were collected and stored until further neurohistochemical analyses.

2.5. [^{18}F]FDG PET neuroimaging

To evaluate brain glucose metabolism, static [^{18}F]FDG PET scans were carried out 3 days after the SE, during the silent period. Protocols for image acquisition and processing have been previously detailed (García-García et al., 2023). A dual PET/CT (computed tomography) scanner was used (Albira scanner, Bruker NMI, Billerica, Massachusetts, U.S.A.). The radiotracer [^{18}F]FDG was injected into the tail vein (approximately 13 MBq–350 μCi-in 0.2 ml of 0.9%; Curium Pharma, Madrid, Spain). Thirty minutes later, rats were anesthetized by isoflurane, placed into the tomograph and the images were acquired. Anesthesia reduces neuronal activity therefore decreasing the [^{18}F]FDG uptake in the rodent brain. However, in static studies, most of the uptake of [^{18}F]FDG occurs in the awake animal within the 30 min before anesthesia (Gold et al., 2018; Matsumura et al., 2003). In addition, brain [^{18}F]FDG uptake by isoflurane-anesthetized rodents has been shown to be the one that most closely reflects the [^{18}F]FDG uptake of awake animals (Bascuñana et al., 2019b; Jahreis et al., 2021).

The tomographic images were reconstructed and processed by PMOD 3.6 software (PMOD Technologies Ltd., Zurich, Switzerland). The steps for quantification of the metabolic activity were the following: (1)

co-registration of the acquired images to a magnetic resonance image (MRI) rat brain template; (2) regional [^{18}F]FDG uptake values acquisition and (3) normalization to the standardized uptake value (SUV, g/ml) based on the animal BW, the dose injected and the corrected [^{18}F]FDG uptake decay as an index of the regional glucose metabolism.

2.6. Neurohistochemical assessments

Rats were sacrificed by decapitation the day after the PET acquisitions. Brains were dissected, cut longitudinally into two halves, frozen on dry ice, and stored at −80 °C. From the left halve of the brain, slices (30 μm-thickness) were collected using a cryostat (Leica CM1850, Leica Biosystems, Germany). Sections containing the hippocampus (6 slices/slide) were thaw-mounted onto Superfrost Plus slides (Thermo Scientific, Germany), dried on a hot plate and stored into slide boxes at −80 °C until the day of the assays.

2.6.1. Nissl staining

Qualitative evaluation of neuronal viability and hippocampal disruption was done with toluidine blue staining. Thus, slides were stained in 0.5% toluidine blue for 1:30 min, decolorized and dehydrated in graded ethanols: (i) 96% ethanol (10 s) and (ii) 100% ethanol (2 × 10 s). Then, the sections were cleared twice (2 min and 5 min) in Neo-Clear™ xylene substitute (Merck-Sigma). Finally, the slides were cover-slipped with DPX mounting medium (Herter, Barcelona, Spain). The images were captured with a digital camera (Leica DFC425, Leica, Germany) coupled to a microscope (Leica DM, 2000 LED, Leica, Germany).

2.6.2. Hippocampal neurodegeneration

Fluoro-Jade C staining was performed following the original protocol (Schmued et al., 2005) with minor modifications. Briefly, The brain sections were fixed in 4% formaldehyde in phosphate buffer pH 7.4 (10 min), rinsed in basic alcohol, 100% ethanol, distilled water, 0.06% potassium permanganate, 0.1% acetic acid solution containing 0.0001% Fluoro-Jade C (Millipore, Darmstadt, Germany), distilled water, and xylene. Then, the slides were cover-slipped with DPX (Herter, Barcelona, Spain). The images were captured with a digital camera (Leica DFC3000G) coupled to a microscope (Leica DM, 2000 LED) by using the FITC filter. At the hippocampal CA1, CA3 and hilus, the fluorescence signal was measured using ImageJ 1.46r software. The average value for each rat was calculated and the results were expressed as percentage *vs* the control group (SAL + VEH).

2.6.3. Reactive astrogliosis

Glial fibrillary acidic protein (GFAP) one-step immunofluorescence was carried out as previously reported (García-García et al., 2023). Briefly, the slices were fixed in 4% formaldehyde in phosphate buffer pH 7.4, washed, and then blocked and permeabilized with 3% BSA, 0.1% Triton X-100 in TBS (60 min). Afterwards, sections were incubated overnight with the anti-GFAP-Cy3 antibody (1:500, Sigma Aldrich) in 1% BSA in TBS at 4 °C. Then, the slides were washed in 0.1% Tween 20 dissolved in TBS (3x for 5 min each) and embedded with home-made Mowiol mounting medium. The images were captured and evaluated using the same optical system used for Fluoro-Jade C, but in this case using the TRITC filter. For each brain section containing the CA1, CA3 and hilus areas at the anterior (dorsal) hippocampus, the fluorescence intensity was measured using ImageJ 1.46r software. As with the Fluoro-Jade C measurements, the average value for each rat was calculated and the results were expressed as percentage *vs* the control group (SAL + VEH).

2.6.4. Microglia-mediated neuroinflammation

In addition, we carried out [^{3}H]PK11195 autoradiography to evaluate the translocator protein (TSPO; 18 kDa), formerly known as the peripheral benzodiazepine receptor (PBR). [^{3}H]PK11195 autoradiography was performed following the protocol previously reported (Foucault-Fruchard et al., 2017) with minor modifications. The slides were dried on a hot plate at 37 °C (10 min), preincubated with 50 mM Tris-HCl pH 7.4 at RT (15 min) and then incubated with 1 nM [^{3}H]PK11195 (PerkinElmer) in preincubation buffer for 60 min. Then, the samples were washed with ice-cold preincubation buffer (2 × 5 min) and dipped in ice-cold distilled water. The slides were air-dried and exposed to Kodak BioMax MR autoradiography film (Carestream, U.S.A.) for approximately 2 months. After manual development, the film was placed onto a light box (Kaiser Prolite 5000, Kaiser Fototechnik, Germany) and the images were captured with a camera (Leica DFC425) coupled to a stereomicroscope (Leica MZ6). The optical density values obtained from the selected brain regions were used as an index of neuroinflammation.

2.7. Statistical analyses

Data from PET and histochemical studies were analyzed by two-way analysis of variance (ANOVA) with pilocarpine and dantrolene treatments as the two main factors. When interaction between factors was significant, further post hoc Tukey tests were performed. The changes on BW vs initial BW were analyzed by two-way ANOVA with repeated measures, with treatments and time as factors followed by post-hoc Tukey test. Mortality rates in pilocarpine treated groups were analyzed by z-test for rates and proportions. In all cases, statistical significance was considered when $p < 0.05$. Data are shown as mean ± SEM. Statistical analyses were performed using SigmaPlot 11.0 software (Systat Software Inc.).

3. Results

Rats in the pilocarpine treated groups reached SE within 34.95 ± 4.29 min. Two rats from the PILO + VEH group (14.3%) and 6 rats from the PILO + DANT group (42.9%) died within the 24h after the SE induced by pilocarpine. Despite the apparent increase in the death rate in the PILO + DANT group, the effect did not reach statistical significance (z-test p = 0.052).

The two-way ANOVA for repeated measures regarding BW changes

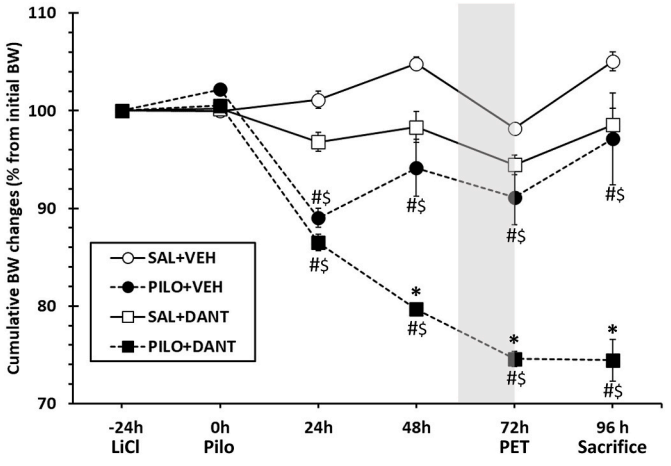

Fig. 1. *Dantrolene aggravated the acute BW loss in response to the SE induced by lithium-pilocarpine further impairing the ability of the rats to recuperate.* Cumulative BW changes throughout the experimental period ranging from the day of LiCl administration (−24h) to the day of sacrifice (+96h) are depicted. BW changes were calculated as a percentage of initial BW (−24h). Shaded area indicates the 12h fasting period before PET acquisitions. Data are shown as mean ± SEM (n = 6–12 rats/group, rats that survived the experimental procedure). Significant differences are depicted as: *p < 0.001 different from PILO + VEH; $^{\#}$p < 0.003 different from initial BW; $^{\$}$p < different from respective control groups, two-way ANOVA followed by post-hoc Tukey tests.

throughout the experimental period (Fig. 1) revealed significant effects of treatment ($p < 0.001$), time ($p < 0.001$) and interaction between treatment and time ($p < 0.001$). Post hoc analyses indicated that, as expected, one day after SE, both PILO + VEH and PILO + DANT rats lost weight ($p < 0.001$ and $p = 0.002$ respectively) in a comparable manner ($p = 0.82$). In the following days, PILO + VEH rats were able to maintain a stable BW gain ending the experiment with a lower BW gain than their respective control SAL + VEH rats (96h, $p = 0.004$). By contrast, dantrolene aggravated the BW loss and PILO + DANT rats ended the experiment with a lower BW gain than PILO + VEH ($p < 0.001$). Dantrolene treatment alone in SAL + DANT rats had no significant effects on BW gain compared with SAL + VEH.

Apart from the hypothalamus and midbrain, a marked hypometabolism measured as standardized uptake value (SUV) was statistically significant in all the epilepsy-related brain areas 3 days after the induction of SE (Fig. 2A). Dantrolene alone (SAL + DANT) had no significant effect on glucose brain metabolism. However, it exacerbated the hypometabolism induced by SE in all areas ($p < 0.001$, Fig. 2A and B).

As can be noticed by the Nissl staining images (Fig. 3), SE resulted in an ostensible reduction in hippocampal neurons at the CA1, hilus and CA3 subregions. Dantrolene alone had no apparent effects either in rats from SAL + DANT or PILO + DANT groups. These qualitative results were in line with and supported by those obtained from Fluoro-Jade C fluorescence labeling (Fig. 4). As expected, Fluoro-Jade C fluorescence labeling revealed no signs of neurodegeneration in SAL + VEH. On the other hand, SE in the PILO + VEH group resulted in significant neurodegeneration in the CA1 ($p < 0.001$), hilus ($p = 0.002$) and CA3 ($p = 0.006$) hippocampal subregions when compared with SAL-VEH. Dantrolene alone had no effects on Fluoro-Jade C labeling, but it significantly exacerbated the neurodegeneration in the PILO + DANT rats ($p < 0.001$ in all three areas).

To investigate the effects of dantrolene on activation of hippocampal astrocytes following lithium-pilocarpine-induced SE, we conducted GFAP immunohistochemistry, measuring the fluorescence signal at the hippocampal hilus (Fig. 5). Astrocytes became activated in response to SE (PILO + VEH) as reflected by the approximately 150% increase in the GFAP fluorescence signal (*vs* SAL + VEH group, $p < 0.001$; Fig. 5B). Even though quantitative measurements were not carried out, Fig. 5A shows that astroglia activation was accompanied by a qualitative apparent thickening of astrocyte bodies and processes. Dantrolene had no effects on astrocytic activation either when administered alone or after pilocarpine.

[^{3}H]PK11195 autoradiography showed that SE resulted in a marked neuroinflammation in all the brain areas analyzed (Fig. 6A). Specifically, at the hippocampus, pilocarpine-induced SE (VEH + PILO) resulted in an increased optical density of 125% compared with the values obtained in the VEH + SAL group ($p < 0.001$; Fig. 6B). Dantrolene by itself had no effects on [^{3}H]PK11195 binding. However, dantrolene administration in rats that underwent SE significantly intensified hippocampal neuroinflammation ($p < 0,005$; Fig. 6B) compared with PILO + VEH group.

4. Discussion

Herein, we report that dantrolene exerts generalized deleterious effects exacerbating the damage induced by SE in the lithium-pilocarpine rat model, contradicting the reported beneficial effects of dantrolene in various animal models of SE.

Epileptogenic activity has been associated with abnormally high $[Ca^{2+}]_i$ levels which acts as a key mediator of excitotoxicity, neuronal cell death and plasticity changes associated with the development of epilepsy (Steinlein, 2014). This $[Ca^{2+}]_i$ increase has been also reported in the rat pilocarpine model of SE (Raza et al., 2001, 2004). Accordingly, therapeutic interventions reducing the elevated $[Ca^{2+}]_i$ have risen as strategies with neuroprotective potential (Steinlein, 2014). In this context, dantrolene acting as a RyR antagonist, and blocking the NMDAR when used at high doses (Obenaus et al., 1989; Salinska et al., 2008), reduces Ca^{2+} influx and mobilization of Ca^{2+} from intracellular stores, making it an attractive potential neuroprotective agent.

In our current study, SE in the PILO + VEH group resulted in short-term brain glucose hypometabolism (Fig. 2), hippocampal neurodegeneration and neuronal death (Figs. 3 and 4), astrogliosis (Fig. 5) and microglia-mediated neuroinflammation (Fig. 6). These results agree with studies reported by other groups (Goffin et al., 2009; Guo et al., 2009; Zhang et al., 2015) as well as by us (García-García et al., 2023; Slowing et al., 2023).

As far as we know, this is the first study that evaluates the effects of dantrolene on brain glucose metabolism during the latent period on the lithium-pilocarpine rat model of SE. Our results consistently show that dantrolene exacerbated most of the signs of damage induced by SE in the PILO + DANT group, including brain glucose hypometabolism that, is not only accepted as an early biomarker of epileptogenesis, but it is also associated to neuronal loss (Dubé et al., 2000), altered neuronal excitability, reduced synaptic density (Kumar and Chugani, 2017a, 2017b), and cerebral hypoperfusion (Bascuñana et al., 2021), among other alterations.

It is well known that neuroinflammation, involving activation of both microglia and astroglia, contributes to the progression of epilepsy in humans (Devinsky et al., 2013) and are hallmarks of TLE in humans (Briellmann et al., 2002; Chauveau et al., 2024; Papadopoulos et al., 2006). Furthermore, these features are reproduced by the pilocarpine models of SE, with lithium (Bulduk et al., 2019; García-García et al., 2023; Slowing et al., 2023) and without (Do Nascimento et al., 2012), as well as by other models of acute seizures (García-García et al., 2018; Jupp et al., 2012). Interestingly, dantrolene exacerbated the effects of SE on microglia-mediated neuroinflammation but not on astrocyte reactivity. In this regard, it is interesting to notice that SE in the rat lithium-pilocarpine model triggers a sequential activation of glial cells. Thus, an early acute activation of microglia (24h) is followed by a later astrocytic activation (Bascuñana et al., 2019a). The lack of effect of dantrolene on SE-induced astroglia reactivity might be explained by this temporal factor. Therefore, we cannot discard that, if assessed later than 4 days after SE, dantrolene might have also increased astroglia reactivity.

The overall deleterious effects of dantrolene were also reflected by the worsening of BW loss in response to SE (Fig. 1), impairing the ability of the animals to respond to the metabolic demands imposed by the SE. Interestingly, dantrolene (15 mg/kg/day x 7days) decreases caloric intake and BW gain in rats allowed to an ad lib high fat diet after a food restriction period (Wires et al., 2017). Even though dantrolene did not reach statistical significance increasing mortality ($p = 0.052$), it is noticeable that the mortality rate after SE increased from 14.3% in the PILO + VEH group to 42.9% in the PILO + DANT group suggesting an additive effect of dantrolene potentiating the mortality induced by pilocarpine.

Our results show a consistent generalized deleterious effect of dantrolene exacerbating the damage induced by SE in the lithium-pilocarpine rat model. Nevertheless, they are difficult to reconcile with the dantrolene's previously reported neuroprotective effects in various models of epileptogenesis. For example, in the kainic acid model of SE, dantrolene (10 mg/kg, i.p.) administrated 30–60 min after kainic acid has shown neuroprotective effects reducing neuronal loss in the hippocampal CA3 (Berg et al., 1995). Likewise, in the electrogenic model of limbic SE, dantrolene (10 mg/kg, i.p.), administered 15 or 140 min after the SE, had time-dependent neuroprotective effects in the hippocampus, being observed when dantrolene was administered 15 min after SE but not after 140 min (Niebauer and Gruenthal, 1999). Besides, neuroprotective effects of dantrolene have been reported in seizures induced by organophosphates (Deshpande et al., 2016) and by TsTX (Nencioni et al., 2004). Regarding the rat pilocarpine model of SE, without lithium pretreatment, neuroprotective effects of dantrolene on CA1 and on CA3 hippocampal areas have also been reported when

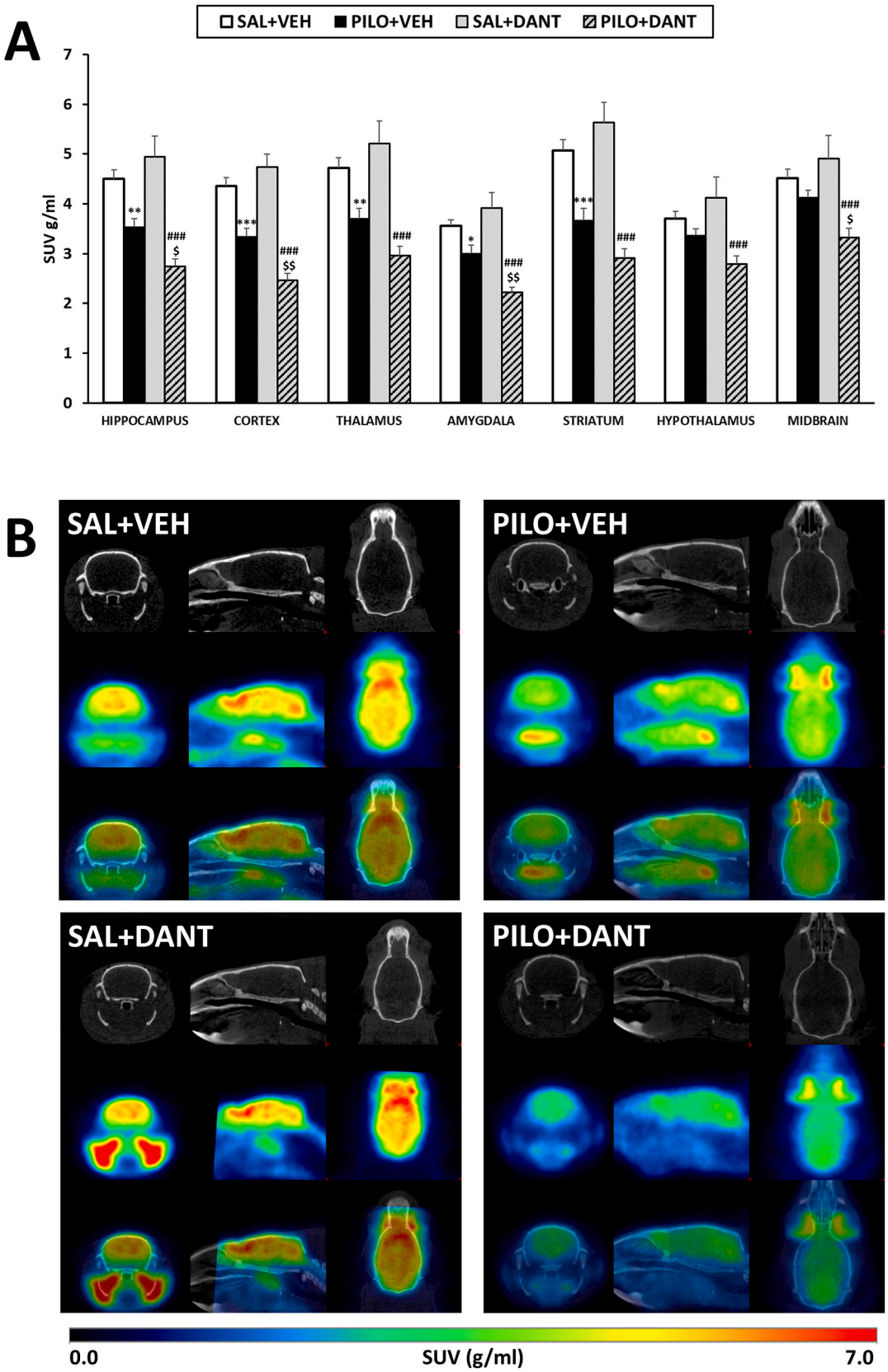

Fig. 2. *SE induced by lithium-pilocarpine in adult male rats led to a significant hypometabolism in key areas known to be involved in epileptogenesis, effect that was exacerbated by dantrolene.* Regional brain glucose metabolism was evaluated by [^{18}F]FDG PET 3 days after the SE. **(A)** Regional brain uptake in the 4 experimental groups is shown as SUV units (mean ± SEM, n = 6–12 rats/group, rats that survived the experimental procedure). **(B)** In each panel: representative CT (upper row), [^{18}F]FDG PET (mid row) and [^{18}F]FDG PET/CT fused images (bottom row) in coronal, sagittal and trans-axial views scaled to SUV of the 4 experimental groups. Significant differences are depicted as: **p < 0.005 PILO + VEH *vs.* SAL + VEH; $^{\#\#\#}$p < 0.001, PILO + DANT *vs* SAL + DANT; $P < 0.05; $^{\$\$}$P < 0.01, PILO + VEH *vs* PILO + DANT, two-way ANOVA followed by post-hoc Tukey tests.

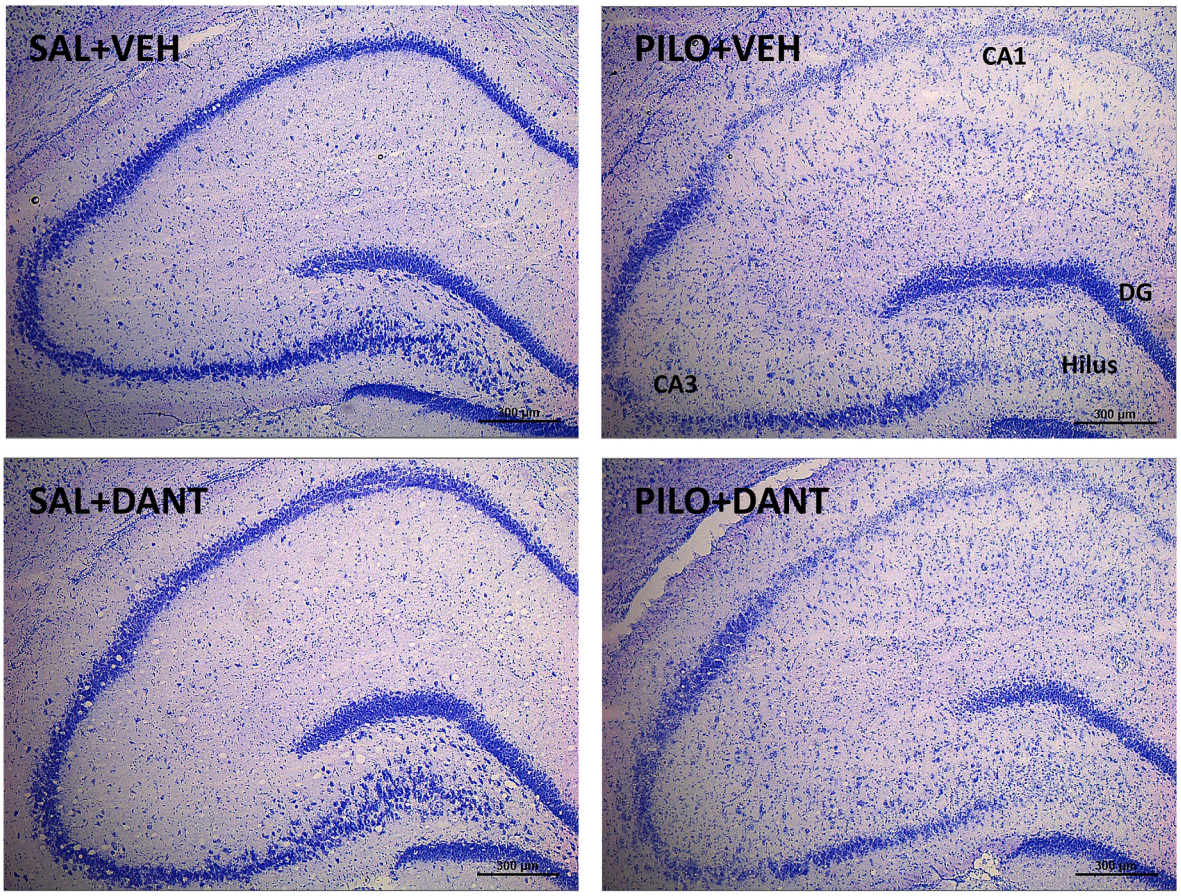

Fig. 3. Nissl *(blue toluidine) staining micrographs from adult male rat brains.* Micrographs illustrate, in a qualitative manner, the damage induced by SE induced by lithium-pilocarpine on the anterior hippocampal areas CA1, CA3 and hilus 3 days after the insult. It can be observed that this effect is aggravated by dantrolene administration.

administered 30 min after the SE (Royero et al., 2020). Yet, none of the abovementioned studies were conducted in the rat lithium-pilocarpine model of SE and it is likely that the intrinsic characteristics of this model might explain, at least partially, these discordant results. Thus, lithium pre-treatment increases sensitivity of muscarinic receptors 1 (M_1) to pilocarpine in rats (Clifford et al., 1987). This heightened pilocarpine sensitivity results in greater IP_3 increase that, through IP_3R, induces Ca^{2+} release from the ER to the cytoplasm (Clifford et al., 1987; Honchar et al., 1983; Sherman et al., 1985). It is interesting to notice that IP_3Rs, but not RyRs, seem to be the major mediator of Ca^{2+} release from stores in the *in vitro* hippocampal neuronal culture (Pal et al., 2001). In this context, dantrolene has been proven ineffective in preventing hippocampal neuronal loss in slices exposed to oxygen-glucose deprivation (Martinez-Sánchez et al., 2004). Likewise, dantrolene does not prevent astroglia reactivity in some epilepsy models involving IP_3R-mediated $[Ca^{2+}]_i$ increase (Ding et al., 2007; Heuser et al., 2018). These data suggest that depending on the model studied, other mechanisms independent of RyRs activation may be involved in mediating $[Ca^{2+}]_i$ increase. In fact, epileptogenic activity has been shown to depend on many mechanisms, including increased hippocampal glutamate levels and NMDAR activation (Nagao et al., 1996; Naylor et al., 2013; Rice and Delorenzo, 1998). The glutamate excitatory signaling pathways and/or IP_3R-mediated $[Ca^{2+}]_i$ increase might play a more significant role than RyRs in the lithium-pilocarpine rat model. Nonetheless, the exacerbated damage induced by post-SE dantrolene is still paradoxical.

Three RyR isoforms (RyR1-3) have been identified (Abu-Omar et al., 2018; Yamaguchi, 2020). Studies in neuronal cultures have shown that the neuroprotective effects of dantrolene mainly relay on the blockade of RyR1 (Mikami et al., 2016). Various RyR2 mutations have been associated with benign epilepsy in children (Ma et al., 2021). However, even though RyR2 is the most predominant isoform in brain (Abu-Omar et al., 2018; Yamaguchi, 2020), it is not blocked by dantrolene (Inan and Wei, 2010; Zhao et al., 2001). Finally, regarding RyR3, studies in animal models of Alzheimer's disease (AD) have shown that up-regulation of RyR3 is neuroprotective (Supnet et al., 2010) and that the RyR3 blockade by dantrolene exacerbates neuronal damage (Zhang et al., 2010). In the same line, it has been suggested that the neuroprotective effects of dantrolene may depend on the stage of AD, being deleterious at the later ones (Liu et al., 2014). Thus, further investigation might be needed to determine the role played by the different RyRs isoforms under neuropathological conditions as well as their regulation by dantrolene.

Again, stressing the potential impact of the methodological differences, it is important to notice that the studies in the aforementioned animal models of epilepsy reporting neuroprotective effects of dantrolene, were carried out with adult Wistar rats (Berg et al., 1995; Nencioni et al., 2004; Niebauer and Gruenthal, 1999; Royero et al., 2020) whereas we have used adult Sprague-Dawley male rats. Importantly, marked rat inter-strain differences have been reported between Wistar and Sprague-Dawley regarding the SE incidence and severity (Langer et al., 2011).

Summing up, our results indicate that post-SE dantrolene administration aggravates the SE-induced neurological damage, contradicting the existing literature. We suggest that the mechanisms underlying the increase in $[Ca^{2+}]_i$ might significantly differ depending on the intrinsic characteristics of the model studied as well as on the methodological conditions. Furthermore, it remains unknown how RyRs are regulated,

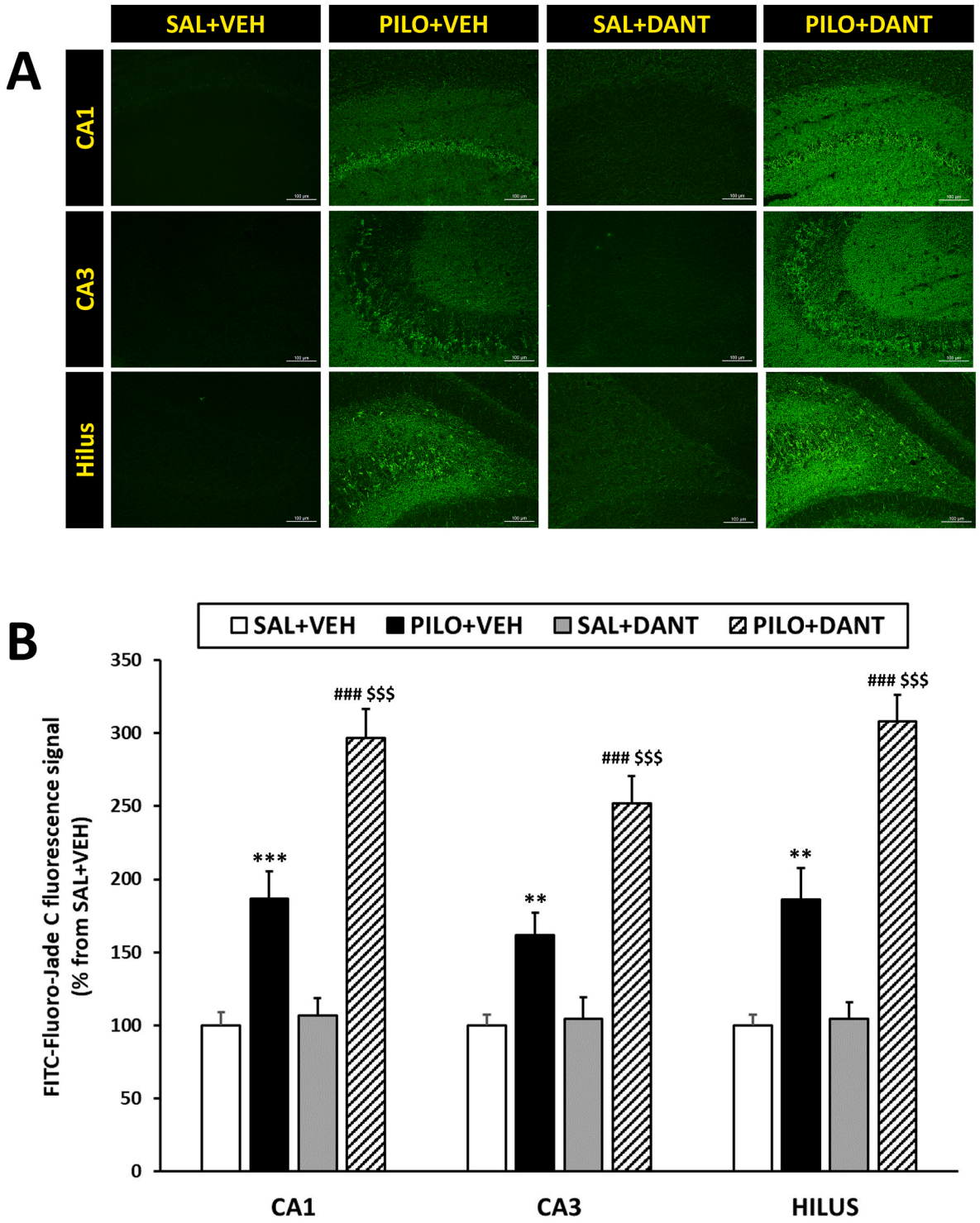

Fig. 4. *Hippocampal neurodegeneration induced by SE is aggravated by dantrolene.* **(A)** Representative images at the level of the CA1 (top row), CA3 (mid row) and dentate gyrus/hilus (bottom row) of the 4 experimental groups. The images show degenerating neurons in PILO + VEH rats 3 days after the SE over an increased FITC fluorescence background signal, and the deleterous effect of dantrolene (PILO + DANT). **(B)** Bar plot corresponding to quantitative data from Fluoro-Jade C fluorecence intensity values as marker of neurodegeration. Data are expressed as percentage of the signal obtained in the SAL + VEH and shown as mean ± SEM (n = 6–12 rats/group; rats that survived the experimental procedure). Significant differences are depicted as: ***p < 0.001, **P < 0.01 SAL + VEH *vs.* PILO + VEH; $^{\#\#\#}$P < 0.001, SAL + DANT *vs.* PILO + DANT and $^{\$\$\$}$p < 0.001, PILO + VEH *vs.* PILO + DANT. two-way ANOVA followed by post-hoc Tukey tests.

and which isoforms of RyR are involved in the process Ca^{2+} -induced release Ca^{2+} from intracellular stores in the lithium-pilocarpine rat model of SE.

CRediT authorship contribution statement

Luis García-García: Writing – original draft, Supervision, Methodology, Investigation, Formal analysis, Conceptualization. **Francisca Gómez-Oliver:** Writing – original draft, Visualization, Formal analysis.

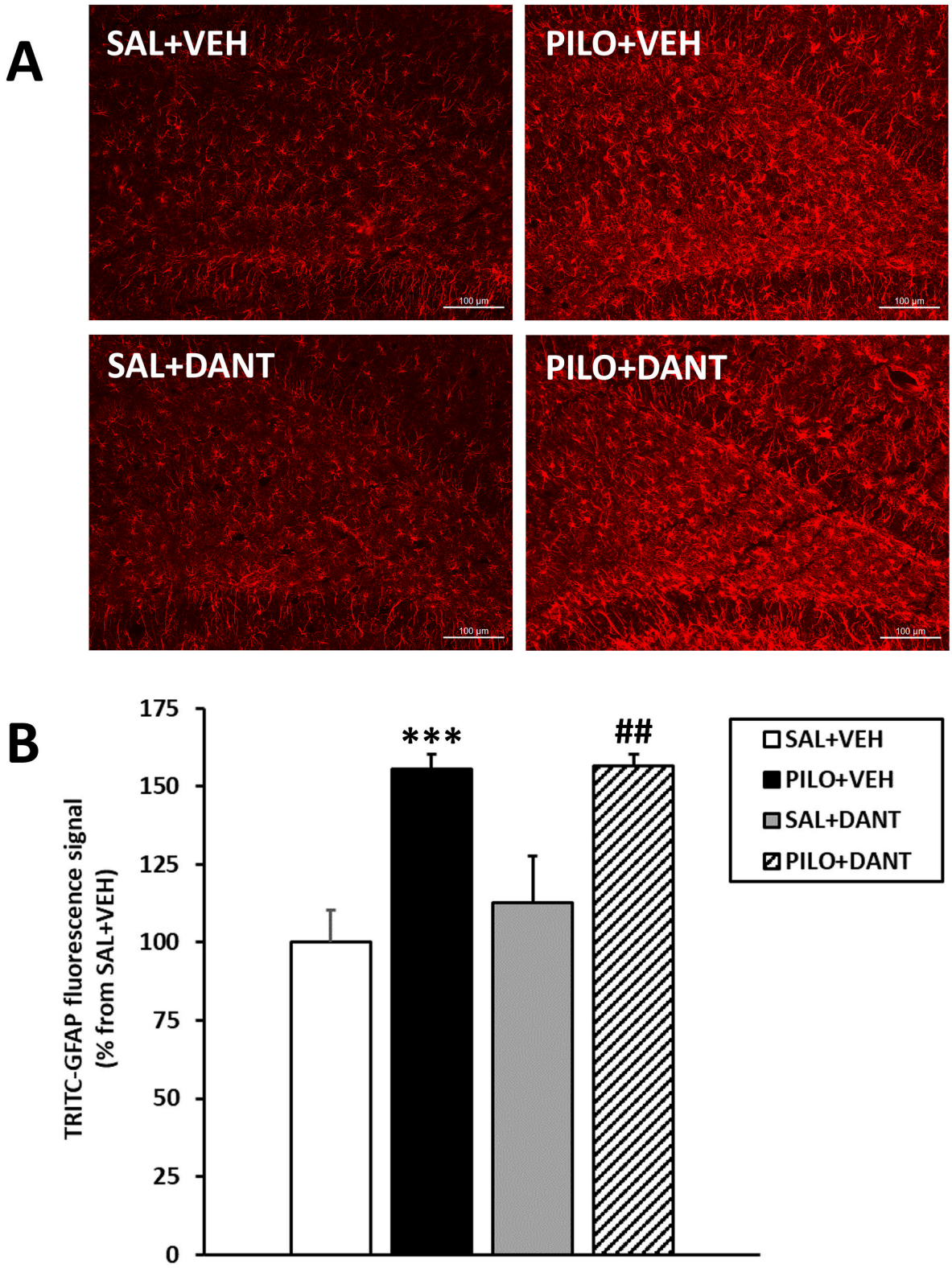

Fig. 5. *Hippocampal astrogliosis induced by SE in the lithium-pilocarpine model was not significantly affected by dantrolene.* **(A)** Images showing representative GFAP immunofluorescence micrographs at the hilus/dentage girus area of the 4 experimental groups. **(B)** Bar plot corresponding to quantitative data from GFAP immunofluorecence intensity as marker of astrogliosis on the hilus. Data are expressed as percentage of the signal obtained in the SAL + VEH group and shown as mean ± SEM (n = 6–12 rats/group; rats that survived the experimental procedure). Significant differences are depicted as ***$p < 0.001$ PILO + VEH *vs.* SAL + VEH and $^{\#\#}p = 0.005$ PILO + DANT *vs.* SAL + DANT, two-way ANOVA followed by post-hoc Tukey tests.

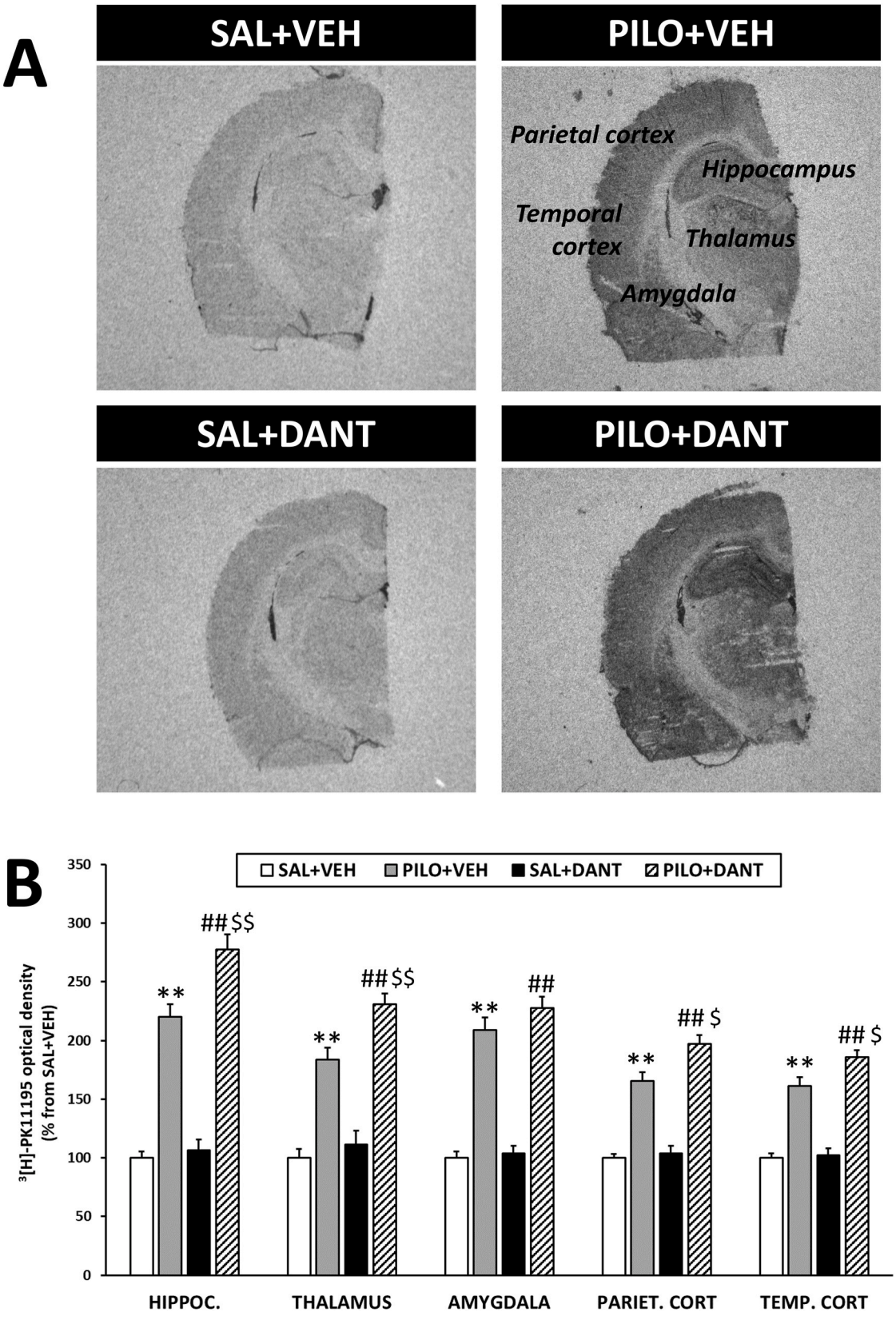

Fig. 6. *Dantrolene treatment exacerbated microglia-induced neuroinflammation in response to the SE in adult male rats as measured by the [^{3}H]PK11195 binding in major brain regions involved in epileptogenesis.* **(A)** Representative [^{3}H]PK11195 autoradiograms corresponding to the 4 experimental groups obtained from both anterior and posterior hippocampus. **(B)** [^{3}H]PK11195 binding expressed in O.D. as the percentage from the SAL + VEH group in various brain regions involved epileptogenesis. Data is shown as mean ± SEM (n = 6–12 rats/group; rats that survived the experimental procedure). $^{**}p < 0.001$, PILO + VEH *vs.* SAL + VEH and $^{\#\#}p < 0.001$ PILO + DANT *vs.* SAL + DANT and $^{\$\$}P < 0.001$, $^{\$}P < 0.005$, PILO + VEH *vs.* PILO + DANT, two-way ANOVA followed by post-hoc Tukey test.

Rubén Fernández de la Rosa: Investigation, Data curation. **Miguel Ángel Pozo:** Supervision, Project administration, Funding acquisition, Conceptualization.

Data availability statement

The datasets used will be available upon reasonable request to the corresponding author.

Ethics approval statement

The study was approved by the Animal Research Ethical Committee of the Universidad Complutense de Madrid and by the Autonomous Community of Madrid (PROEX 222.1/20), and it was carried out in accordance with regulations of the European Union (2010/63/UE) and Spain (RD53/2013) regarding animal welfare. All efforts were made to minimize, as much as possible, both the number of animals used and their suffering.

We confirm that we have read the Journal's position on issues involved in ethical publication and affirm that this report is consistent with those guidelines.

Declaration of competing interest

None of the authors has any conflict of interest to disclose.

Acknowledgments

Deep thanks are given to Dr. Mercedes Delgado for her invaluable technical assistance with this study. This work was financially supported by the Spanish Ministerio de Ciencia e Innovación (Retos PID2019-106968RB-100).

Data availability

Data will be made available on request.

References

Abu-Omar, N., Das, J., Szeto, V., Feng, Z.P., 2018. Neuronal ryanodine receptors in development and aging. Mol. Neurobiol. 55, 1183–1192. https://doi.org/10.1007/S12035-016-0375-4.

Ahmed Juvale, I.I., Che Has, A.T., 2020. The evolution of the pilocarpine animal model of status epilepticus. Heliyon 6, e04557. https://doi.org/10.1016/J.HELIYON.2020.E04557.

Bascuñana, P., Gendron, T., Sander, K., Jahreis, I., Polyak, A., Ross, T.L., Bankstahl, M., Arstad, E., Bankstahl, J.P., 2019a. Ex vivo characterization of neuroinflammatory and neuroreceptor changes during epileptogenesis using candidate positron emission tomography biomarkers. Epilepsia 60, 2325–2333. https://doi.org/10.1111/EPI.16353.

Bascuñana, P., Thackeray, J.T., Bankstahl, M., Bengel, F.M., Bankstahl, J.P., 2019b. Anesthesia and preconditioning induced changes in mouse brain [18F] FDG uptake and kinetics. Mol. Imag. Biol. 21, 1089–1096. https://doi.org/10.1007/s11307-019-01314-9.

Bascuñana, P., Wolf, B.J., Jahreis, I., Brackhan, M., García-García, L., Ross, T.L., Bengel, F.M., Bankstahl, M., Bankstahl, J.P., 2021. 99mTc-HMPAO SPECT imaging reveals brain hypoperfusion during status epilepticus. Metab. Brain Dis. 36, 2597–2602. https://doi.org/10.1007/S11011-021-00843-Z.

Berg, M., Bruhn, T., Frandsen, A., Schousboe, A., Diemer, N.H., 1995. Kainic acid-induced seizures and brain damage in the rat: role of calcium homeostasis. J. Neurosci. Res. 40, 641–646. https://doi.org/10.1002/jnr.490400509.

Brandt, C., Töllner, K., Klee, R., Bröer, S., Löscher, W., 2015. Effective termination of status epilepticus by rational polypharmacy in the lithium-pilocarpine model in rats: window of opportunity to prevent epilepsy and prediction of epilepsy by biomarkers. Neurobiol. Dis. 75, 78–90. https://doi.org/10.1016/J.NBD.2014.12.015.

Briellmann, R.S., Kalnins, R.M., Berkovic, S.F., Jackson, G.D., 2002. Hippocampal pathology in refractory temporal lobe epilepsy: T2-weighted signal change reflects dentate gliosis. Neurology 58, 265–271. https://doi.org/10.1212/WNL.58.2.265.

Bulduk, E.B., Kurt, G., Barun, S., Aydemir, O., Kiziltas, M., Oktem, M., Turhan, T., Atilla, P., Muftuoglu, S., 2019. The effects of minocycline on the Hippocampus in lithium- pilocarpine induced status epilepticus in rat: relations with microglial/astrocytic activation and serum S100B level. Turk Neurosurg 29 (1), 95–105. https://doi.org/10.5137/1019-5149.JTN.22744-18.

Chauveau, F., Winkeler, A., Chalon, S., Boutin, H., Becker, G., 2024. PET imaging of neuroinflammation: any credible alternatives to TSPO yet? Mol. Psychiatr. https://doi.org/10.1038/S41380-024-02656-9.

Clifford, D.B., Olney, J.W., Maniotis, A., Collins, R.C., Zorumski, C.F., 1987. The functional anatomy and pathology of lithium-pilocarpine and high-dose pilocarpine seizures. Neuroscience 23, 953–968. https://doi.org/10.1016/0306-4522(87)90171-0.

DeLorenzo, R.J., Pal, S., Sombati, S., 1998. Prolonged activation of the N-methyl-D-aspartate receptor-Ca2+ transduction pathway causes spontaneous recurrent epileptiform discharges in hippocampal neurons in culture. Proc. Natl. Acad. Sci. U. S. A. 95, 14482–14487. https://doi.org/10.1073/PNAS.95.24.14482.

Deshpande, L.S., Blair, R.E., Phillips, K.F., DeLorenzo, R.J., 2016. Role of the calcium plateau in neuronal injury and behavioral morbidities following organophosphate intoxication. Ann. N. Y. Acad. Sci. 1374, 176–183. https://doi.org/10.1111/nyas.13122.

Devinsky, O., Vezzani, A., Najjar, S., De Lanerolle, N.C., Rogawski, M.A., 2013. Glia and epilepsy: excitability and inflammation. Trends Neurosci. 36, 174–184. https://doi.org/10.1016/J.TINS.2012.11.008.

Ding, S., Fellin, T., Zhu, Y., Lee, S.Y., Auberson, Y.P., Meaney, D.F., Coulter, D.A., Carmignoto, G., Haydon, P.G., 2007. Enhanced astrocytic Ca2+ signals contribute to neuronal excitotoxicity after status epilepticus. J. Neurosci. 27, 10674–10684. https://doi.org/10.1523/JNEUROSCI.2001-07.2007.

Do Nascimento, A.L., Dos Santos, N.F., Campos Pelágio, F., Aparecida Teixeira, S., De Moraes Ferrari, E.A., Langone, F., 2012. Neuronal degeneration and gliosis time-course in the mouse hippocampal formation after pilocarpine-induced status epilepticus. Brain Res. 1470, 98–110. https://doi.org/10.1016/J.BRAINRES.2012.06.008.

Dubé, C., Marescaux, C., Nehlig, A., 2000. A metabolic and neuropathological approach to the understanding of plastic changes that occur in the immature and adult rat brain during lithium-pilocarpine-induced epileptogenesis. Epilepsia 41. https://doi.org/10.1111/j.1528-1157.2000.tb01554.x.

Fisher, R.S., Cross, J.H., French, J.A., Higurashi, N., Hirsch, E., Jansen, F.E., Lagae, L., Moshé, S.L., Peltola, J., Roulet Perez, E., Scheffer, I.E., Zuberi, S.M., 2017. Operational classification of seizure types by the international league against epilepsy: position paper of the ILAE commission for classification and terminology. Epilepsia 58, 522–530. https://doi.org/10.1111/EPI.13670.

Foucault-Fruchard, L., Doméné, A., Page, G., Windsor, M., Emond, P., Rodrigues, N., Dollé, F., Damont, A., Buron, F., Routier, S., Chalon, S., Antier, D., 2017. Neuroprotective effect of the alpha 7 nicotinic receptor agonist PHA 543613 in an in vivo excitotoxic adult rat model. Neuroscience 356, 52–63. https://doi.org/10.1016/j.neuroscience.2017.05.019.

García-García, L., Fernández de la Rosa, R., Delgado, M., Silván, Á., Bascuñana, P., Bankstahl, J.P., Gomez, F., Pozo, M.A., 2018. Metyrapone prevents acute glucose hypermetabolism and short-term brain damage induced by intrahippocampal administration of 4-aminopyridine in rats. Neurochem. Int. 113, 92–106. https://doi.org/10.1016/j.neuint.2017.11.018.

García-García, L., Gomez, F., Delgado, M., Fernández de la Rosa, R., Pozo, M.Á., 2023. The vasodilator naftidrofuryl attenuates short-term brain glucose hypometabolism in the lithium-pilocarpine rat model of status epilepticus without providing neuroprotection. Eur. J. Pharmacol. 939. https://doi.org/10.1016/J.EJPHAR.2022.175453.

Goffin, K., Paesschen, W. Van, Dupont, P., Laere, K. Van, 2009. Longitudinal microPET imaging of brain glucose metabolism in rat lithium-pilocarpine model of epilepsy. Exp. Neurol. 217, 205–209. https://doi.org/10.1016/J.EXPNEUROL.2009.02.008.

Gold, M.E.L., Norell, M.A., Budassi, M., Vaska, P., Schulz, D., 2018. Rapid 18F-FDG uptake in brain of awake, behaving rat and anesthetized chicken has implications for behavioral PET studies in species with high metabolisms. Front. Behav. Neurosci. 12, 115. https://doi.org/10.3389/fnbeh.2018.00115.

Guo, Y., Gao, F., Wang, S., Ding, Y., Zhang, H., Wang, J., Ding, M.P., 2009. In vivo mapping of temporospatial changes in glucose utilization in rat brain during epileptogenesis: an 18F-fluorodeoxyglucose-small animal positron emission tomography study. Neuroscience 162, 972–979. https://doi.org/10.1016/j.neuroscience.2009.05.041.

Heuser, K., Nome, C.G., Pettersen, K.H., Åbjørsbråten, K.S., Jensen, V., Tang, W., Sprengel, R., Taubøll, E., Nagelhus, E.A., Enger, R., 2018. Ca2+ signals in astrocytes facilitate spread of epileptiform activity. Cerebr. Cortex 28, 4036–4048. https://doi.org/10.1093/CERCOR/BHY196.

Honchar, M.P., Olney, J.W., Sherman, W.R., 1983. Systemic cholinergic agents induce seizures and brain damage in lithium-treated rats. Science 220, 323–325. https://doi.org/10.1126/SCIENCE.6301005.

Inan, S., Wei, H., 2010. The cytoprotective effects of dantrolene: a ryanodine receptor antagonist. Anesth. Analg. 111, 1400–1410. https://doi.org/10.1213/ANE.0B013E3181F7181C.

Jahreis, I., Bascuñana, P., Ross, T.L., Bankstahl, J.P., Bankstahl, M., 2021. Choice of anesthesia and data analysis method strongly increases sensitivity of 18F-FDG PET imaging during experimental epileptogenesis. PLoS One 16. https://doi.org/10.1371/JOURNAL.PONE.0260482.

Janszky, J., Janszky, I., Schulz, R., Hoppe, M., Behne, F., Pannek, H.W., Ebner, A., 2005. Temporal lobe epilepsy with hippocampal sclerosis: predictors for long-term surgical outcome. Brain 128, 395–404. https://doi.org/10.1093/brain/awh358.

Jupp, B., Williams, J., Binns, D., Hicks, R.J., Cardamone, L., Jones, N., Rees, S., O'Brien, T.J., 2012. Hypometabolism precedes limbic atrophy and spontaneous recurrent seizures in a rat model of TLE. Epilepsia 53, 1233–1244. https://doi.org/10.1111/J.1528-1167.2012.03525.X.

Kumar, A., Chugani, H.T., 2017a. The role of radionuclide imaging in epilepsy, part 2: epilepsy syndromes. J. Nucl. Med. Technol. 45, 294–301. https://doi.org/10.2967/jnumed.113.129593.

Kumar, A., Chugani, H.T., 2017b. The role of radionuclide imaging in epilepsy, part 1: sporadic temporal and extratemporal lobe epilepsy. J. Nucl. Med. Technol. 45, 286–293. https://doi.org/10.2967/jnumed.112.114397.

Langer, M., Brandt, C., Löscher, W., 2011. Marked strain and substrain differences in induction of status epilepticus and subsequent development of neurodegeneration, epilepsy, and behavioral alterations in rats. [corrected]. Epilepsy Res. 96, 207–224. https://doi.org/10.1016/J.EPLEPSYRES.2011.06.005.

Lee, E.M., Park, G.Y., Im, K.C., Kim, S.T., Woo, C.-W., Chung, J.H., Kim, K.S., Kim, J.S., Shon, Y.-M., Kim, Y.I., Kang, J.K., 2012. Changes in glucose metabolism and metabolites during the epileptogenic process in the lithium-pilocarpine model of epilepsy. Epilepsia 53, 860–869. https://doi.org/10.1111/j.1528-1167.2012.03432.x.

Liu, J., Supnet, C., Sun, S., Zhang, H., Good, L., Popugaeva, E., Bezprozvanny, I., 2014. The role of ryanodine receptor type 3 in a mouse model of Alzheimer disease. Channels 8, 230–242. https://doi.org/10.4161/CHAN.27471.

Ma, M.G., Liu, X.R., Wu, Y., Wang, J., Li, B.M., Shi, Y.W., Su, T., Li, B., Liu, D.T., Yi, Y.H., Liao, W.P., 2021. RYR2 mutations are associated with benign epilepsy of childhood with centrotemporal spikes with or without arrhythmia. Front. Neurosci. 15. https://doi.org/10.3389/FNINS.2021.629610.

Martinez-Sánchez, M., Striggow, F., Schröder, U.H., Kahlert, S., Reymann, K.G., Reiser, G., 2004. Na(+) and Ca(2+) homeostasis pathways, cell death and protection after oxygen-glucose-deprivation in organotypic hippocampal slice cultures. Neuroscience 128, 729–740. https://doi.org/10.1016/J.NEUROSCIENCE.2004.06.074.

Matsumura, A., Mizokawa, S., Tanaka, M., Wada, Y., Nozaki, S., Nakamura, F., Shiomi, S., Ochi, H., Watanabe, Y., 2003. Assessment of microPET performance in analyzing the rat brain under different types of anesthesia: comparison between quantitative data obtained with microPET and ex vivo autoradiography. Neuroimage 20, 2040–2050. https://doi.org/10.1016/j.neuroimage.2003.08.020.

McDonald, J.W., Fix, A.S., Tizzano, J.P., Schoepp, D.D., 1993. Seizures and brain injury in neonatal rats induced by 1S,3R-ACPD, a metabotropic glutamate receptor agonist. J. Neurosci. 13, 4445–4455. https://doi.org/10.1523/JNEUROSCI.13-10-04445.1993.

Mikami, Y., Kanemaru, K., Okubo, Y., Nakaune, T., Suzuki, J., Shibata, K., Sugiyama, H., Koyama, R., Murayama, T., Ito, A., Yamazawa, T., Ikegaya, Y., Sakurai, T., Saito, N., Kakizawa, S., Iino, M., 2016. Nitric oxide-induced activation of the type 1 ryanodine receptor is critical for epileptic seizure-induced neuronal cell death. EBioMedicine 11, 253–261. https://doi.org/10.1016/J.EBIOM.2016.08.020.

Mori, F., Okada, M., Tomiyama, M., Kaneko, S., Wakabayashi, K., 2005. Effects of ryanodine receptor activation on neurotransmitter release and neuronal cell death following kainic acid-induced status epilepticus. Epilepsy Res. 65, 59–70. https://doi.org/10.1016/J.EPLEPSYRES.2005.04.006.

Nagao, T., Alonso, A., Avoli, M., 1996. Epileptiform activity induced by pilocarpine in the rat hippocampal-entorhinal slice preparation. Neuroscience 72, 399–408. https://doi.org/10.1016/0306-4522(95)00534-X.

Nagarkatti, N., Deshpande, L.S., Carter, D.S., Delorenzo, R.J., 2010. Dantrolene inhibits the calcium plateau and prevents the development of spontaneous recurrent epileptiform discharges following in vitro status epilepticus. Eur. J. Neurosci. 32, 80–88. https://doi.org/10.1111/j.1460-9568.2010.07262.x.

Naylor, D.E., Liu, H., Niquet, J., Wasterlain, C.G., 2013. Rapid surface accumulation of NMDA receptors increases glutamatergic excitation during status epilepticus. Neurobiol. Dis. 54, 225–238. https://doi.org/10.1016/J.NBD.2012.12.015.

Nencioni, A.L.A., Lebrun, I., Dorce, V.A.C., 2004. Dantrolene protects hippocampal cells from damage induced by TsTX, an α-scorpion toxin from Tityus serrulatus. Toxicon 44, 179–183. https://doi.org/10.1016/j.toxicon.2004.05.018.

Niebauer, M., Gruenthal, M., 1999. Neuroprotective effects of early vs. late administration of dantrolene in experimental status epilepticus. Neuropharmacology 38, 1343–1348. https://doi.org/10.1016/S0028-3908(99)00059-3.

Obenaus, A., Mody, I., Baimbridge, K.G., 1989. Dantrolene-Na (Dantrium) blocks induction of long-term potentiation in hippocampal slices. Neurosci. Lett. 98, 172–178. https://doi.org/10.1016/0304-3940(89)90505-3.

O'Brien, T.J., Miles, K., Ware, R., Cook, M.J., Binns, D.S., Hicks, R.J., 2008. The cost-effective use of 18F-FDG PET in the presurgical evaluation of medically refractory focal epilepsy. J. Nucl. Med. 49, 931–937. https://doi.org/10.2967/jnumed.107.048207.

Pal, S., Sun, D., Limbrick, D., Rafiq, A., DeLorenzo, R.J., 2001. Epileptogenesis induces long-term alterations in intracellular calcium release and sequestration mechanisms in the hippocampal neuronal culture model of epilepsy. Cell Calcium 30, 285–296. https://doi.org/10.1054/CECA.2001.0236.

Papadopoulos, V., Baraldi, M., Guilarte, T.R., Knudsen, T.B., Lacapère, J.J., Lindemann, P., Norenberg, M.D., Nutt, D., Weizman, A., Zhang, M.R., Gavish, M., 2006. Translocator protein (18kDa): new nomenclature for the peripheral-type benzodiazepine receptor based on its structure and molecular function. Trends Pharmacol. Sci. 27, 402–409. https://doi.org/10.1016/J.TIPS.2006.06.005.

Pitkänen, A., 2002. Drug-mediated neuroprotection and antiepileptogenesis: animal data. Neurology 59. https://doi.org/10.1212/WNL.59.9_SUPPL_5.S27.

Popescu, B.O., Oprica, M., Sajin, M., Stanciu, C.L., Bajenaru, O., Predescu, A., Vidulescu, C., Popescu, L.M., 2002. Dantrolene protects neurons against kainic acid induced apoptosis in vitro and in vivo. J. Cell Mol. Med. 6, 555–569. https://doi.org/10.1111/j.1582-4934.2002.tb00454.x.

Racine, R.J., 1972. Modification of seizure activity by electrical stimulation. II. Motor seizure. Electroencephalogr. Clin. Neurophysiol. 32, 281–294. https://doi.org/10.1016/0013-4694(72)90177-0.

Raza, M., Blair, R.E., Sombati, S., Carter, D.S., Deshpande, L.S., DeLorenzo, R.J., 2004. Evidence that injury-induced changes in hippocampal neuronal calcium dynamics during epileptogenesis cause acquired epilepsy. Proc. Natl. Acad. Sci. U. S. A. 101, 17522–17527. https://doi.org/10.1073/pnas.0408155101.

Raza, M., Pal, S., Rafiq, A., DeLorenzo, R.J., 2001. Long-term alteration of calcium homeostatic mechanisms in the pilocarpine model of temporal lobe epilepsy. Brain Res. 903, 1–12. https://doi.org/10.1016/S0006-8993(01)02127-8.

Rice, A.C., Delorenzo, R.J., 1998. NMDA receptor activation during status epilepticus is required for the development of epilepsy. Brain Res. 782, 240–247. https://doi.org/10.1016/S0006-8993(97)01285-7.

Rigoulot, M.A., Koning, E., Ferrandon, A., Nehlig, A., 2004. Neuroprotective properties of topiramate in the lithium-pilocarpine model of epilepsy. J. Pharmacol. Exp. Therapeut. 308, 787–795. https://doi.org/10.1124/JPET.103.057091.

Rossi, A.R., Angelo, M.F., Villarreal, A., Lukin, J., Ramos, A.J., 2013. Gabapentin administration reduces reactive gliosis and neurodegeneration after pilocarpine-induced status epilepticus. PLoS One 8. https://doi.org/10.1371/JOURNAL.PONE.0078516.

Royero, P.X., Higa, G.S.V., Kostecki, D.S., dos Santos, B.A., Almeida, C., Andrade, K.A., Kinjo, E.R., Kihara, A.H., 2020. Ryanodine receptors drive neuronal loss and regulate synaptic proteins during epileptogenesis. Exp. Neurol. 327. https://doi.org/10.1016/j.expneurol.2020.113213.

Salinska, E., Sobczuk, A., Lazarewicz, J.W., 2008. Dantrolene antagonizes the glycineB site of the NMDA receptor. Neurosci. Lett. 432, 137–140. https://doi.org/10.1016/J.NEULET.2007.12.013.

Schmued, L.C., Stowers, C.C., Scallet, A.C., Xu, L., 2005. Fluoro-Jade C results in ultra high resolution and contrast labeling of degenerating neurons. Brain Res. 1035, 24–31. https://doi.org/10.1016/J.BRAINRES.2004.11.054.

Sherman, W.R., Munsell, L.Y., Gish, B.G., Honchar, M.P., 1985. Effects of systemically administered lithium on phosphoinositide metabolism in rat brain, kidney, and testis. J. Neurochem. 44, 798–807. https://doi.org/10.1111/J.1471-4159.1985.TB12886.X.

Slowing, K., Gomez, F., Delgado, M., Fernández De La Rosa, R., Hernández-Martín, N., Pozo, M.Á., García-García, L., 2023. PET imaging and neurohistochemistry reveal that curcumin attenuates brain hypometabolism and hippocampal damage induced by status epilepticus in rats. Planta Med. 89, 364–376. https://doi.org/10.1055/A-1948-4378.

Steinlein, O.K., 2014. Calcium signaling and epilepsy. Cell Tissue Res. 357, 385–393. https://doi.org/10.1007/s00441-014-1849-1.

Supnet, C., Noonan, C., Richard, K., Bradley, J., Mayne, M., 2010. Up-regulation of the type 3 ryanodine receptor is neuroprotective in the TgCRND8 mouse model of Alzheimer's disease. J. Neurochem. 112, 356–365. https://doi.org/10.1111/J.1471-4159.2009.06487.X.

Tang, F., Hartz, A.M.S., Bauer, B., 2017. Drug-resistant epilepsy: multiple hypotheses, few answers. Front. Neurol. 8. https://doi.org/10.3389/FNEUR.2017.00301.

Turski, W.A., Cavalheiro, E.A., Schwarz, M., Czuczwar, S.J., Kleinrok, Z., Turski, L., 1983. Limbic seizures produced by pilocarpine in rats: behavioural, electroencephalographic and neuropathological study. Behav. Brain Res. 9, 315–335. https://doi.org/10.1016/0166-4328(83)90136-5.

Walton, N.Y., Treiman, D.M., 1988. Response of status epilepticus induced by lithium and pilocarpine to treatment with diazepam. Exp. Neurol. 101, 267–275. https://doi.org/10.1016/0014-4886(88)90010-6.

Wires, E.S., Trychta, K.A., Bäck, S., Sulima, A., Rice, K.C., Harvey, B.K., 2017. High fat diet disrupts endoplasmic reticulum calcium homeostasis in the rat liver. J. Hepatol. 67, 1009–1017. https://doi.org/10.1016/J.JHEP.2017.05.023.

Yamaguchi, N., 2020. Molecular insights into calcium dependent regulation of ryanodine receptor calcium release channels. Adv. Exp. Med. Biol. 1131, 321–336. https://doi.org/10.1007/978-3-030-12457-1_13.

Yang, H.S., Choi, J.M., In, J., Sung, T.Y., Kim, Y.B., Sultana, S., 2023. Current clinical application of dantrolene sodium. Anesthesiol. Pain Med. 18, 220–232. https://doi.org/10.17085/APM.22260.

Yang, Y., Guo, Y., Kuang, Y., Wang, Shan, Jiang, Y., Ding, Y., Wang, Shuang, Ding, M., 2014. Serotonin 1A receptor inhibits the status epilepticus induced by lithium-pilocarpine in rats. Neurosci. Bull. 30, 401–408. https://doi.org/10.1007/s12264-013-1396-x.

Yoshida, M., Sakai, T., 2006. Dantrolene, a calcium-induced calcium release inhibitor, prevents the acquisition of amygdaloid kindling in rats, a model of experimental epilepsy. Tohoku J. Exp. Med. 209, 303–310. https://doi.org/10.1620/TJEM.209.303.

Zhang, H., Sun, S., Herreman, A., De Strooper, B., Bezprozvanny, I., 2010. Role of presenilins in neuronal calcium homeostasis. J. Neurosci. 30, 8566–8580. https://doi.org/10.1523/JNEUROSCI.1554-10.2010.

Zhang, L., Guo, Y., Hu, H., Wang, J., Liu, Z., Gao, F., 2015. FDG-PET and NeuN-GFAP immunohistochemistry of hippocampus at different phases of the pilocarpine model of temporal lobe epilepsy. Int. J. Med. Sci. 12, 288–294. https://doi.org/10.7150/IJMS.10527.

Zhao, F., Li, P., Chen, S.R.W., Louis, C.F., Fruen, B.R., 2001. Dantrolene inhibition of ryanodine receptor Ca2+ release channels. Molecular mechanism and isoform selectivity. J. Biol. Chem. 276, 13810–13816. https://doi.org/10.1074/JBC.M006104200.